Pacific Journal of Mathematics

MINIMAL SOLUTIONS TO THE LOCAL CAPILLARY WEDGE PROBLEM

ROBERT HUFF

Volume 224 No. 2 April 2006

PACIFIC JOURNAL OF MATHEMATICS
Vol. 224, No. 2, 2006

MINIMAL SOLUTIONS TO THE LOCAL CAPILLARY WEDGE PROBLEM

ROBERT HUFF

We give sufficient conditions for the existence of minimal capillary graphs over quadrilaterals symmetric with respect to a diagonal. The proof is constructive, making use of the Weierstrass representation theorem for minimal surfaces. In the process, we construct minimal solutions to the local capillary wedge problem for any wedge angle $0 < \phi < \pi$ and contact angles $\gamma_1, \gamma_2 \in (0, \pi)$ such that $|\gamma_1 - \gamma_2| \leq \pi - \phi$. When $|\gamma_1 - \gamma_2| < \pi - \phi$, the solution presented here has a jump discontinuity at the wedge corner.

1. Introduction and statement of results

Given a convex quadrilateral Q (each interior angle strictly less than π) with edges $\{s_k\}_{k=1}^4$, and given *contact angles* $\{\gamma_k\}_{k=1}^4$, we ask under what conditions there exists a corresponding *capillary graph*, that is, a minimal surface that is a graph over Q (except perhaps at the vertices) and that meets each wall $s_k \times \mathbb{R}$ at a constant angle γ_k. We will give sufficient conditions in the case where Q is symmetric with respect to a diagonal.

Physically, a capillary graph models the behavior of a surface formed by a liquid in a container, which in our case is a cylinder with quadrilateral cross section. In the absence of gravity any such graph given by u satisfies

$$\operatorname{div} \frac{\operatorname{grad} u}{\sqrt{1 + |\operatorname{grad} u|^2}} = H \qquad \text{in } Q,$$

$$\left\langle \frac{\operatorname{grad} u}{\sqrt{1 + |\operatorname{grad} u|^2}}, \nu_k \right\rangle = \cos \gamma_k \quad \text{along } s_k,$$

where ν_k is the outward pointing unit normal to s_k and H is a constant. The first equation means the graph has constant mean curvature H, and the second is just the contact angle condition along the edges.

MSC2000: primary 76B45; secondary 53A10.
Keywords: capillary graph, contact angle, minimal surface, Weierstrass representation, quadrilateral.

The wedge problem. A necessary condition for the existence of a capillary graph over a convex quadrilateral comes from the local capillary wedge problem, which deals with the existence of capillary graphs defined locally in a neighborhood of a wedge vertex. In this setting, Concus and Finn [1996] have shown it is not possible for a capillary graph with constant mean curvature to exist if the contact angles (γ_1, γ_2) along the two sides of the wedge are such that

$$|\gamma_1 + \gamma_2 - \pi| > \phi.$$

where $\phi \in (0, \pi)$ is the wedge angle. The forbidden region thus defined is the union $\mathscr{D}_1^+ \cup \mathscr{D}_1^-$ in Figure 1. Thus, a minimal capillary graph over a convex quadrilateral can exist only if

$$(\gamma_k, \gamma_{k+1}) \notin \mathscr{D}_1^+ \cup \mathscr{D}_1^- \ \text{ with respect to } \alpha_k, \quad k = 1, 2, 3, 4,$$

where α_k is the interior angle between s_k and s_{k+1} and $k = 4$ implies $k + 1 = 1$.

Also labeled in Figure 1 are the regions

$$\mathscr{R} = \{(\gamma_1, \gamma_2) : |\gamma_1 + \gamma_2 - \pi| < \phi \text{ and } |\gamma_1 - \gamma_2| < \pi - \phi\},$$
$$\mathscr{D}_2^+ \cup \mathscr{D}_2^- = \{(\gamma_1, \gamma_2) : |\gamma_1 - \gamma_2| > \pi - \phi\}.$$

By considering portions of planes and spheres over linear wedges, one can see that a solution to the local capillary problem (in zero gravity) exists for any $(\gamma_1, \gamma_2) \in \mathscr{R}$ and any mean curvature value H. According to a conjecture by Concus and Finn [1996], existence for any H should also hold in the closure of $\mathscr{D}_2^\pm$. Here, we make progress towards this conjecture by proving the following theorem, establishing

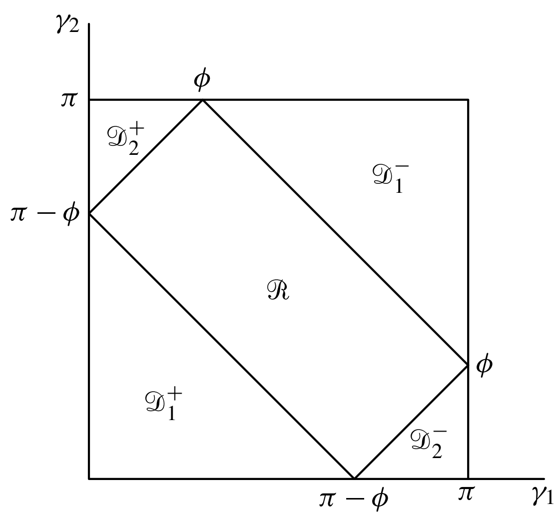

Figure 1. Contact angle diagram.

existence in the closure of $\mathfrak{D}_2^\pm$ minus the points where either γ_1 or γ_2 equals 0 or π. Because of the geometric nature of our construction, we are also able to determine the behavior of the solutions at the wedge corner.

Theorem 1. *There is a minimal solution to the local capillary wedge problem for any wedge angle* $0 < \phi < \pi$ *and contact angle pair*

$$(\gamma_1, \gamma_2) \in \overline{\mathfrak{D}}_2^\pm$$

with respect to ϕ *such that* $0 < \gamma_1, \gamma_2 < \pi$. *Moreover, if* (γ_1, γ_2) *lies in the interior* $\mathring{\mathfrak{D}}_2^\pm$ *of* $\mathfrak{D}_2^\pm$, *a solution exists with a finite jump discontinuity.*

Finn [1996] showed existence for any $H \neq 0$ in $\overline{\mathfrak{D}}_2^\pm - \overline{\mathfrak{D}}_1^\pm$ so long as the wedge angle is less than 31.5°. Combining this with the theorem, we obtain:

Corollary. *There is a solution to the local capillary wedge problem for any mean curvature value* H *and any* $(\gamma_1, \gamma_2) \in \overline{\mathfrak{D}}_2^\pm$ *such that* $0 < \gamma_1, \gamma_2 < \pi$ *so long as the wedge angle is less than* 31.5°.

Note. Crenshaw and Lancaster [2006] have proved Theorem 1 for wedge angles $\pi/2 < \phi < \pi$ and contact angles $(\gamma_1, \gamma_2) \in \mathring{\mathfrak{D}}_2^\pm$, by solving an appropriate Riemann–Hilbert problem.

Statement of the global existence theorem. Theorem 1 will arise as a corollary of Theorem 2 below, concerning the global existence of minimal capillary graphs over convex quadrilaterals. Unfortunately, it is too ambitious at this point to consider general convex quadrilaterals; instead, we restrict our attention to those that are symmetric with respect to a diagonal. To prove Theorem 2, we use the Weierstrass representation theorem for minimal surfaces to construct the graph; the sufficient conditions we derive for global existence result from studying the Gauss map on the graph.

Let Q be a convex quadrilateral that is symmetric with respect to a diagonal. Orient Q in the xy-plane so that the line of symmetry is the x-axis, and label the edges s_1, s_2, s_3, s_4 along with the wedge angle ϕ between s_1 and s_2 as shown in Figure 2. Next, assume the existence of a minimal capillary graph over Q having contact angle γ_k along the edge s_k. Furthermore, assume that the portion of the x-axis contained in Q, labeled b in Figure 2, is contained in the graph. By the Schwarz reflection principle for minimal surfaces, this last assumption implies the graph is symmetric with respect to 180° rotation around b, and this symmetry of the graph results in a symmetry of the contact angles:

$$\gamma_3 = \pi - \gamma_1 \quad \text{and} \quad \gamma_4 = \pi - \gamma_2. \tag{1}$$

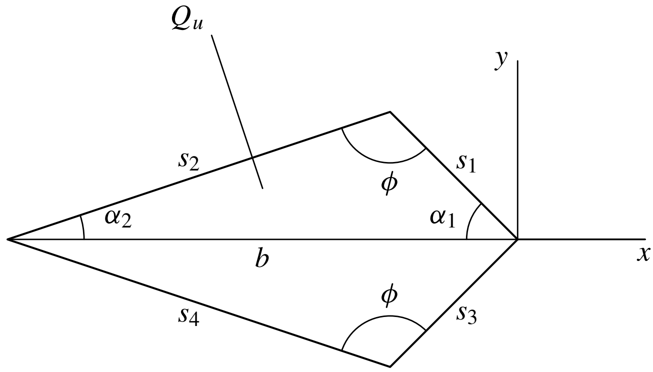

Figure 2. The quadrilateral Q oriented in the xy-plane.

Theorem 2. *Let Q, oriented and labeled as in Figure 2, be any convex quadrilateral symmetric with respect to the x-axis. Let $0 < \gamma_1, \gamma_2 < \pi$ and set $\gamma_3 = \pi - \gamma_1$, $\gamma_4 = \pi - \gamma_2$. Suppose further that*

$$(\gamma_1, \gamma_2) \in \overline{\mathcal{D}}_2^{\pm}$$

with respect to the wedge angle ϕ between s_1 and s_2. Then there exists a minimal capillary graph over Q with contact angle γ_k on the edge s_k, $k = 1, 2, 3, 4$. Furthermore, if

$$(\gamma_1, \gamma_2) \in \mathring{\mathcal{D}}_2^{\pm},$$

a solution exists with a finite jump discontinuity at the vertices $s_1 \cap s_2$ and $s_3 \cap s_4$.

Note that under the hypotheses of the theorem, we also have $(\gamma_3, \gamma_4) \in \overline{\mathcal{D}}_2^{\pm}$ with respect to ϕ, by symmetry.

Before proving Theorem 2, we recall the Weierstrass representation theorem for minimal surfaces.

2. Background

The Weierstrass representation. Given a domain $\Omega \subset \mathbb{C}$, the Weierstrass representation theorem says that any (orientation preserving) conformal minimal immersion

$$X = (X_1, X_2, X_3) : \Omega \to \mathbb{R}^3$$

can be expressed, up to translation, in terms of a meromorphic function g and a holomorphic one-form dh by the formula

$$X(z) = \operatorname{Re} \int_{\cdot}^{z} \left(\frac{1}{2}(g^{-1} - g)\, dh,\ \frac{i}{2}(g^{-1} + g)\, dh,\ dh \right), \tag{2}$$

where g is the stereographic projection of the Gauss map and

$$dh = \left(\frac{\partial X_3}{\partial x} - i\frac{\partial X_3}{\partial y}\right) dz$$

is called the complex height differential (note that $\operatorname{Re} dh = dX_3$). Conversely, the theorem states that if g is a meromorphic function and dh a holomorphic one-form on Ω such that dh has a zero of order n at z if and only if g has a zero or pole of order n at z, then (2) gives an (orientation preserving) conformal minimal immersion on Ω that is well-defined provided that

$$\operatorname{Re}\int_c \left(\frac{1}{2}(g^{-1}-g)\,dh,\ \frac{i}{2}(g^{-1}+g)\,dh,\ dh\right) = 0$$

for every simple closed curve $c \subset \Omega$. (This condition is satisfied automatically if Ω is simply connected.)

Determining dh via the second fundamental form. For a minimal surface given by Weierstrass data g and dh, we have, for tangent vectors v and w,

$$\frac{dg(v)\,dh(w)}{g} = \mathrm{II}(v, w) - i\,\mathrm{II}(v, iw),$$

where II is the second fundamental form on the surface (see [Hoffman and Karcher 1997] for details). Therefore:

$$\text{(3)} \qquad c \text{ is a principal curve} \iff \frac{dg(\dot{c})\,dh(\dot{c})}{g} \in \mathbb{R};$$

$$\text{(4)} \qquad c \text{ is an asymptotic curve} \iff \frac{dg(\dot{c})\,dh(\dot{c})}{g} \in i\mathbb{R}.$$

We see from (3) and (4) that the function ζ given by

$$\text{(5)} \qquad \zeta(z) = \int_{\cdot}^{z} \sqrt{\frac{dg\,dh}{g}}$$

maps principal curves into vertical or horizontal lines and asymptotic curves into lines of slope ± 1. The map ζ is called the *developing map* of the one-form $\sqrt{dg\,dh/g}$. It is a local isometry between the minimal surface equipped with the conformal cone metric $|dg\,dh/g|$ and the Euclidean plane.

Each surface considered will have boundary consisting of principal and asymptotic curves, which will allow us to determine the function ζ. Once this is done, we can use (5) to conclude that

$$dh = \frac{g(d\zeta)^2}{dg}.$$

3. Proof of Theorem 2

Determining the image of the Gauss map. To construct the desired capillary graph in $\mathbb{R}^3$, we will find a parametrization of its image Ω under the Gauss map. Because of symmetry it is sufficient to consider the graph over the triangle Q_u with base b and base angles α_1 and α_2 (see Figure 2). From now on we assume without loss of generality, thanks to (1), that $\gamma_1 \le \gamma_2$ and $\gamma_1 \le \pi/2$. It will be convenient to distinguish two cases:

$$0 < \gamma_1 \le \pi/2 \le \gamma_2 < \pi, \tag{C1}$$

$$0 < \gamma_1 \le \gamma_2 \le \pi/2. \tag{C2}$$

We can also exclude the situation $\gamma_1 = \gamma_2 = \pi/2$, since then the desired graph is just part of a horizontal plane.

Because of the contact angle conditions, the Gauss map takes the interior of an edge s_k into (part of) a circle C_k on the sphere. Under stereographic projection, C_k is described as follows:

If $\gamma_k \ne \pi/2$, the circle C_k is the boundary of the disk

$$D_k = D(\sec\gamma_k\, e^{i\theta_k}, |\tan\gamma_k|) \tag{7}$$

of radius $|\tan\gamma_k|$ and center $\sec\gamma_k\, e^{i\theta_k}$, where

$$\theta_1 = \pi/2 - \alpha_1, \quad \theta_2 = \pi/2 + \alpha_2. \tag{8}$$

If $\gamma_k = \pi/2$, then C_k is the line through the origin in the direction of s_k and we define D_k as one of the half-planes bounded by this line: in case (C1),

$$D_1 = \bigcup_{0<\gamma<\pi/2} D(\sec\gamma\, e^{i\theta_1}, |\tan\gamma|)$$

or

$$D_2 = \bigcup_{\pi/2<\gamma<\pi} D(\sec\gamma\, e^{i\theta_2}, |\tan\gamma|);$$

in case (C2),

$$D_2 = \bigcup_{0<\gamma<\pi/2} D(\sec\gamma\, e^{i\theta_2}, |\tan\gamma|).$$

Finally, we note that the Gauss map takes the edge b into a segment of the imaginary axis, which we again label b.

In case (C1) we take the Gauss image Ω to be the region common to $\mathbb{C} - \bar{D}_1$, $\mathbb{C} - \bar{D}_2$, the half-plane $\{x > 0\}$, and the unit disk $D(0, 1)$, while in case (C2) we take Ω to be the region common to the exterior of the smaller disk D_1, the interior of the larger disk D_2, the half-plane $\{x > 0\}$, and the unit disk. We now show that these descriptions make sense under the hypotheses of Theorem 2. The circle C_k,

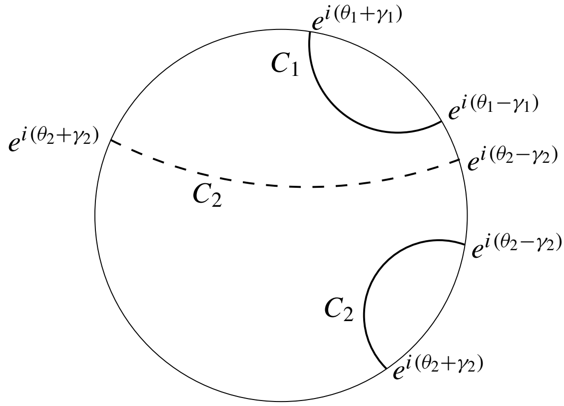

Figure 3. Intersections of C_1 and C_2 with the unit circle. The solid-line C_2 corresponds to case (C1), while the dashed-line C_2 corresponds to case (C2).

$k = 1, 2$, intersects the unit circle at $e^{i(\theta_k \pm \gamma_k)}$. Referring to Figure 3, we see that

$$\begin{aligned}
(\gamma_1, \gamma_2) \in \bar{\mathscr{D}}_2^\pm \text{ with respect to } \phi &\iff \gamma_2 - \gamma_1 \geq \alpha_1 + \alpha_2 = \pi - \phi \\
&\iff \pi/2 + \alpha_2 - \gamma_2 \leq \pi/2 - \alpha_1 - \gamma_1 \\
&\iff \theta_2 - \gamma_2 \leq \theta_1 - \gamma_1 \\
&\iff \begin{cases} D_1 \cap D_2 = \varnothing & \text{in case (C1)}, \\ C_1 \subset \bar{D}_2 & \text{in case (C2)}, \end{cases}
\end{aligned}$$

as required. Thus the Gauss image Ω is the stated intersection. More explicitly, Ω is the region bounded by a curvilinear polygon consisting of the contact-angle arcs C_1, C_2, the segment b of the imaginary axis, and up to three arcs of the unit circle, labeled a_1, a_2, a_3 in the order shown in Figure 4, left. Each a_k present on $\partial\Omega$ comes from a finite jump discontinuity (a vertical line segment) over a vertex. Arc a_2 is present if and only if $(\gamma_1, \gamma_2) \in \mathring{\mathscr{D}}_2^\pm$ with respect to ϕ; the arc (a_1 or a_3) connecting C_k to b is present if and only if $(\gamma_k, \pi - \gamma_k) \in \mathring{\mathscr{D}}_2^\pm$ with respect to $2\alpha_k$. Note that from now on we use C_1 and C_2 to refer to arcs on the boundary of Ω, rather than whole circles.

Since Ω only depends on the contact angles and the interior angles of the triangle Q_u, we will construct graphs over one triangle per similarity class. To deal with other triangles in a congruence class, we simply apply a homothety of $\mathbb{R}^3$ to the graph, which changes the edge lengths of the triangle but preserves minimality and contact angles.

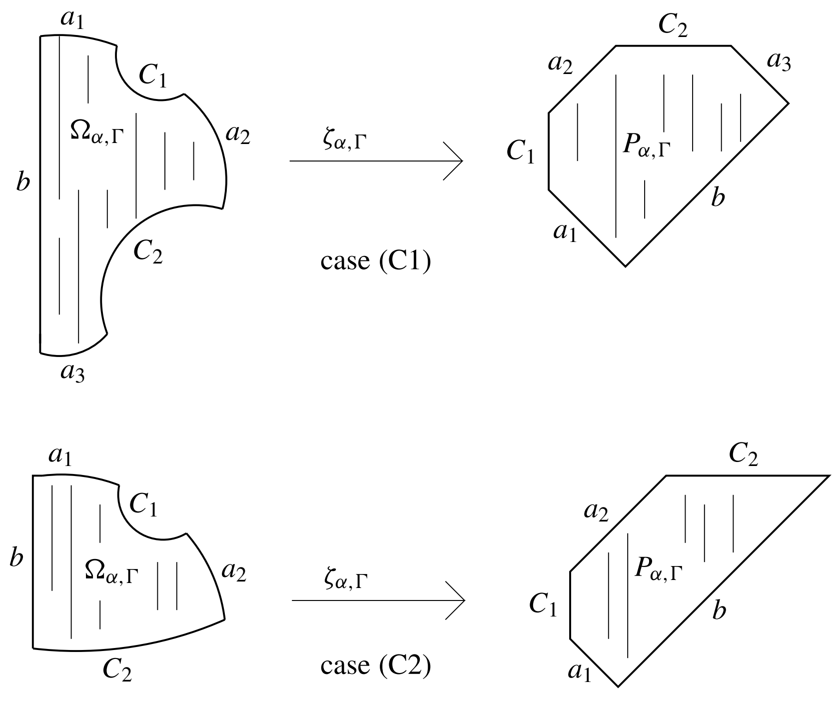

Figure 4. The developing map $\zeta_{\alpha,\Gamma}$.

We now seek to parametrize the capillary graph via the inverse of its Gauss map. The stereographic projection of the Gauss map of a minimal surface is conformal and orientation preserving, so its inverse can be expressed in terms of Weierstrass data g and dh using formula (2) above, where in our case $g(z) = z$ by construction. Hence, it remains to determine dh, which we will do in terms of the developing map of the complexified second fundamental form. Thus we need to investigate what properties this map should satisfy. It will sometimes be convenient to write $\Omega_{\alpha,\Gamma}$ instead of Ω, where we have set

$$\Gamma = (\gamma_1, \gamma_2) \quad \text{and} \quad \alpha = (\alpha_1, \alpha_2).$$

Existence of the developing map. Consider the function $\zeta = \zeta_{\alpha,\Gamma}$ on $\Omega_{\alpha,\Gamma}$ given by (5). Each edge a_k corresponds to an asymptotic curve, because ζ maps it into a vertical line over a vertex of Q_u. It follows from (4) that the image of each such edge under ζ is a segment of slope ± 1. Edges C_1 and C_2 correspond to the contact curves, which are planar curves along which the graph meets the plane of the curve at a constant angle. By Joachimstahl's Theorem, these are principal curves, so it follows from (3) that they are mapped by ζ into horizontal or vertical lines. We conclude that ζ maps $\Omega_{\alpha,\Gamma}$ conformally onto a Euclidean polygon $P_{\alpha,\Gamma}$. Diagrams of this map when $\Omega_{\alpha,\Gamma}$ contains the maximum number of edges — six in case (C1) and five in case (C2) — are shown in Figure 4. Thus we have reduced our task to proving that such a map always exists, for an appropriate choice of the Euclidean polygon $P_{\alpha,\Gamma}$.

We do this using a continuity argument and certain properties of extremal length, which we record here in the context of interest; for more generality and proofs, see [Ahlfors 1973]. Given a curvilinear polygon Δ, a Borel-measurable function $\rho > 0$ on Δ defines a conformal metric $\rho(dx^2 + dy^2)$. The *extremal length* between two edges A and B of Δ, or (A, B)-extremal length, is defined as

$$\mathrm{Ext}_{A,B}(\Delta) := \sup_{\rho} \frac{(\inf_{\gamma} \rho\text{-length of } \gamma)^2}{\rho\text{-area of } \Delta},$$

where the infimum is over all curves $\gamma : [0, 1] \to \Delta$ such that $\gamma(0) \in A,\ \gamma(1) \in B$, and $\gamma(t) \subset \mathring{\Delta}$ for $t \in (0, 1)$. Extremal length is invariant under biholomorphisms and has the following properties:

(i) If A and B are adjacent, $\mathrm{Ext}_{A,B}(\Delta) = 0$.

(ii) If B is degenerate (a point) and $\mathrm{dist}(A, B) > 0$, then $\mathrm{Ext}_{A,B}(\Delta) = \infty$.

(iii) If Δ is a Euclidean rectangle with edges $\{B_k\}$, $k = 1, 2, 3, 4$,

$$\mathrm{Ext}_{B_1,B_3}(\Delta) = \frac{1}{\mathrm{Ext}_{B_2,B_4}(\Delta)} = \frac{|B_2|}{|B_1|},$$

where the bars denote Euclidean length.

(iv) If $\Delta_1 \subset \Delta_2$ are such that edges $A_k, B_k \subset \Delta_k$, $k = 1, 2$, satisfy $A_1 \subset A_2$ and $B_1 \subset B_2$, then

$$\mathrm{Ext}_{A_2,B_2}(\Delta_2) \le \mathrm{Ext}_{A_1,B_1}(\Delta_1),$$

and the inequality is strict if $A_1 \ne A_2$ or $B_1 \ne B_2$.

(v) $\mathrm{Ext}_{A,B}(\Delta)$ depends continuously on the edge lengths of Δ.

We will prove the existence of $P_{\alpha,\Gamma}$ and the required biholomorphic map ζ in case (C1), assuming that a_1, a_2, a_3 are nondegenerate, as in Figure 4 (top). The proofs of the remaining cases are similar and simpler.

Consider the space $\mathcal{P}_6$ of Euclidean hexagons P as in Figure 4, normalized so that $C_1 \cap a_1 = 0 \in \mathbb{C}$ and $|C_1| = 1$. Any polygon $P \in \mathcal{P}_6$ is uniquely determined by the three (Euclidean) edge lengths $|a_1|, |a_2|, |C_2|$. This allows us to parametrize $\mathcal{P}_6$ using $(|a_1|, |a_2|, |C_2|)$ as coordinates:

$$P = P(|a_1|, |a_2|, |C_2|).$$

Choose any $|a_1|, |a_2|$ that are the first two coordinates of some $P \in \mathcal{P}_6$. Allowing $|C_2|$ to vary, we see that as $|C_2|$ approaches its lower limit (which is zero), the edges a_3 and a_2 become adjacent. By property (i) above, the (a_2, a_3)-extremal length tends to 0. Inversely, as $|C_2|$ approaches its upper limit, a_3 degenerates to a point and property (ii) says that $\mathrm{Ext}_{a_2,a_3}(P) \to \infty$. By the continuity property (v), there exists an intermediate $|\hat{C}_2| = f_1(|a_1|, |a_2|)$ such that

$$\mathrm{Ext}_{a_2,a_3}(\Omega_{\alpha,\Gamma}) = \mathrm{Ext}_{a_2,a_3}\big(P(|a_1|, |a_2|, f_1(|a_1|, |a_2|))\big)\,. \tag{9}$$

Claim 1. *The function f_1 is continuous.*

Proof. Suppose f_1 is not continuous at some point $a = (|a_1|, |a_2|)$. Then we can find a subsequence $a_k \to a$ such that $f_1(a_k)$ converges to some $|C_2'| \neq f_1(a)$. Since extremal length depends continuously on edge lengths (property (v) above), it follows that $\mathrm{Ext}_{a_2,a_3}\big(P(a_k, f_1(a_k))\big)$ converges to $\mathrm{Ext}_{a_2,a_3}\big(P(a, |C_2'|)\big)$, and equation (9) tells us that $\mathrm{Ext}_{a_2,a_3}\big(P(a, |C_2'|)\big) = \mathrm{Ext}_{a_2,a_3}(\Omega_{a,\Gamma}) = \mathrm{Ext}_{a_2,a_3}\big(P(a, f_1(a))\big)$. However, since $|C_2'| \neq f_1(a)$, property (iv) implies that $\mathrm{Ext}_{a_2,a_3}\big(P(a, |C_2'|)\big) \neq \mathrm{Ext}_{a_2,a_3}\big(P(a, f_1(a))\big)$, a contradiction. □

Continuing, fix a length $|a_1|$ and consider $P = P(|a_1|, |a_2|, f_1(|a_1|, |a_2|))$. As $|a_2|$ approaches its lower limit of zero, property (ii) on the previous page says that

$$\mathrm{Ext}_{a_2,b}(P) \to \infty.$$

As $|a_2|$ approaches its upper limit of infinity, it is also true that $|b|$ approaches infinity. Therefore, consider a rectangle $R = R(|a_1|, |a_2|)$ with opposite sides $e_1 \subset a_2$ and $e_2 \subset b$ such that $|e_k| \to \infty$ $(k = 1, 2)$ as $|a_2| \to \infty$. Then property (iii) implies that $\mathrm{Ext}_{e_1,e_2}(R) \to 0$ as $|a_2|$ approaches infinity, and property (iv) shows that

$$\mathrm{Ext}_{a_2,b}(P) \to 0$$

as $|a_2|$ approaches infinity. By the continuity of f_1, there exists an intermediate $|\hat{a}_2| = f_2(|a_1|)$ such that

$$\mathrm{Ext}_{a_2,b}(\Omega_{\alpha,\Gamma}) = \mathrm{Ext}_{a_2,b}\big(P(|a_1|,\ f_2(|a_1|),\ f_1(|a_1|, f_2(|a_1|)))\big)\,. \tag{10}$$

The continuity of f_2 is crucial to the remainder of the proof, and we prove it now.

Claim 2. *The function f_2 is continuous.*

Proof. As in the proof of Claim 1, we assume f_2 is discontinuous at some point $|a_1|$. We can find a subsequence $|a_1^k| \to |a_1|$ such that $f_2(|a_1^k|)$ converges to some $|a_2'| \neq f_2(|a_1|)$.

Let P and P' be the hexagons corresponding to $f_2(|a_1|)$ and $|a_2'|$, respectively. If the jump from $f_2(|a_1|)$ to $|a_2'|$ is a decrease, there are two possibilities: Either P' is strictly contained in P, or P' is such that there is a jump increase in $|b|$.

In the first case, it follows from property (iv) that $\mathrm{Ext}_{a_2,b}(P') > \mathrm{Ext}_{a_2,b}(P)$, so that equation (10) does not hold at P', a contradiction.

In the second case, we first decrease P' to a hexagon P'' by shortening the edges C_2 and b so that the edge a_3 of P'' is contained in the edge a_3 of P. By property (iv), we have $\mathrm{Ext}_{a_2,a_3}(P') > \mathrm{Ext}_{a_2,a_3}(P'')$. Another application of (iv) shows that $\mathrm{Ext}_{a_2,a_3}(P'') > \mathrm{Ext}_{a_2,a_3}(P)$, and hence that $\mathrm{Ext}_{a_2,a_3}(P') > \mathrm{Ext}_{a_2,a_3}(P)$. This implies that (9) is not satisfied at P', a contradiction.

Similarly, we reach contradictions if the jump from $f_2(|a_1|)$ to a_2' is an increase. Thus, we have shown that f_2 is continuous. □

Finally, we let $|a_1|$ vary within the family of polygons

$$P = P\big(|a_1|,\ f_2(|a_1|),\ f_1(|a_1|, f_2(|a_1|))\big).$$

As $|a_1|$ approaches its lower limit of zero, it follows from (9) and (10) that P approaches a pentagon with $|a_1| = 0$ and all other lengths nonzero. Thus,

$$\mathrm{Ext}_{b,C_1}(P) \to 0$$

as $|a_1|$ approaches zero.

As $|a_1|$ approaches infinity, consider the renormalized hexagon

$$P' = |a_1|^{-1} P\big(|a_1|, f_2(|a_1|), f_1(|a_1|, f_2(|a_1|))\big),$$

which has the properties that $|a_1| = 1$ and $|C_1|$ approaches zero as $|a_1|$ approaches infinity. Since extremal length is a conformal invariant, equations (9) and (10) also hold in P'. Now, if $|b|$ in P' approaches infinity as $|a_1|$ approaches infinity, it follows from the geometry of the hexagons that $|a_2|$ must also approach infinity. In such a case, we can apply properties (iii) and (iv) from page 255 to show that $\mathrm{Ext}_{a_2,b}(P')$ approaches zero as $|a_1|$ approaches infinity, violating the condition that equation (10) be satisfied. Thus, $|b|$ must be bounded in the family $\{P'\}$, and hence

$$\mathrm{Ext}_{b,C_1}(P') = \mathrm{Ext}_{b,C_1}\big(P(|a_1|, f_2(|a_1|), f_1(|a_1|, f_2(|a_1|)))\big) \to \infty$$

as $|a_1|$ approaches infinity. By the continuity of f_1 and f_2, there is an intermediate $|\hat{a}_1|$ such that $\hat{P} := P(|\hat{a}_1|, f_2(|\hat{a}_1|),\ f_1(|\hat{a}_1|, f_2(|\hat{a}_1|)))$ satisfies

$$\mathrm{Ext}_{b,C_1}(\Omega_{\alpha,\Gamma}) = \mathrm{Ext}_{b,C_1}(\hat{P})\,. \tag{11}$$

From the Riemann mapping theorem and the fact that $\partial\Omega_{\alpha,\Gamma}$ and $\partial\hat{P}$ are simple closed curves, it follows that there is a biholomorphic map ζ between $\Omega_{\alpha,\Gamma}$ and $\hat{P}$, and we can normalize so that

$$\zeta(a_2 \cap C_1) = a_2 \cap C_1,\quad \zeta(a_2 \cap C_2) = a_2 \cap C_2 \ \text{ and } \ \zeta(a_3 \cap C_2) = a_3 \cap C_2. \tag{12}$$

Since (9) is satisfied and extremal length is invariant under biholomorphisms, property (iv) implies that

$$\zeta(a_3 \cap b) = a_3 \cap b.$$

Given this and the equality $\mathrm{Ext}_{a_2,b}(\Omega_{\alpha,\Gamma}) = \mathrm{Ext}_{a_2,b}(\hat{P})$ arising from (10), we get

$$\zeta(a_1 \cap b) = a_1 \cap b,$$

which in turn, together with $\mathrm{Ext}_{a_2,a_3}(\Omega_{\alpha,\Gamma}) = \mathrm{Ext}_{a_2,a_3}(\hat{P})$ from (11), shows that

$$\zeta(a_1 \cap C_1) = a_1 \cap C_1.$$

Thus, the function ζ is the desired $\zeta_{\alpha,\Gamma}$ and the polygon $\hat{P}$ is the desired $P_{\alpha,\Gamma}$.

Verification of the parametrizations. With the existence of the map $\zeta = \zeta_{\alpha,\Gamma}$, we obtain a parametrization on $\Omega = \Omega_{\alpha,\Gamma}$ of a minimal surface given by Weierstrass data

$$g(z) = z \quad \text{and} \quad dh = \frac{g(d\zeta)^2}{dg}.$$

It now needs to be checked this surface is indeed a graph with the desired properties.

Choosing a base point $z_0 \in \Omega$ and using the formulas immediately above, the parametrization (2) takes the form

$$X(z) = \mathrm{Re} \int_{z_0}^{z} (1 - z^2, i(1 + z^2), 2z) \frac{(d\zeta)^2}{2\,dz}.$$

So that the resulting quadrilateral will be oriented and labeled as in Figure 2, we choose $z_0 = a_1 \cap b$ or $z_0 = C_1 \cap b$ if a_1 is not present in Ω.

Now, the map X is continuous on $\overline{\Omega}$. To see this, take a vertex v of Ω and denote the angle at v, $\zeta(v)$, by φ, ψ, respectively. Then, near v we have

$$\zeta(z) = \zeta(v) + (z - v)^{\psi/\varphi} \zeta_0(z),$$

where ζ_0 is holomorphic and nonzero at v. Thus, $\zeta'(z)^2 = (z - v)^{2(\psi/\varphi - 1)} \zeta_1(z)$, where ζ_1 is holomorphic and nonzero at v. It is easily verified that $\psi/\varphi > \frac{1}{2}$. Hence,

$$2\Big(\frac{\psi}{\varphi} - 1\Big) > -1,$$

and it follows that

$$\frac{(d\zeta)^2}{dz} = (\zeta')^2\, dz$$

is integrable on $\overline{\Omega}_\Gamma$. Therefore,

X is continuous on $\overline{\Omega}$.

To analyze X on $\partial\Omega$, we parametrize C_k counterclockwise by

$$z_k(t) = \sec(\gamma_k) e^{i\theta_k} + |\tan \gamma_k| e^{it} \quad \text{if } \gamma_k \neq \pi/2,$$

and by

$$z_k(t) = \pm e^{i(\theta_k - \pi/2)} t \quad \text{if } \gamma_k \neq \pi/2,$$

where the sign factor is negative if $k = 2$ in case (C1), and positive otherwise (compare the definition of D_k on page 252). Since ζ maps C_1 into a vertical line and C_2 into a horizontal line, we have

$$(-1)^k d\zeta(\dot{z}_k)^2 > 0. \tag{13}$$

If $\gamma_k \neq \pi/2$, then $dz(\dot{z}_k) = i\,|\tan\gamma_k|\,e^{it}$ and we have

$$|\tan\gamma_k| = (-1)^{k-1}\tan\gamma_k \text{in case (C1).}$$

Thus, in this case we compute

(14)

$$\begin{aligned}
dX_1(\dot{z}_k) &= \operatorname{Re}\left((1-z_k^2)\frac{d\zeta(\dot{z}_k)^2}{2\,dz(\dot{z}_k)}\right)\\
&= \frac{d\zeta(\dot{z}_k)^2}{2}\operatorname{Re}\left(\frac{1-\sec^2(\gamma_k)e^{i2\theta_k}-2\sec\gamma_k\,|\tan\gamma_k|e^{i(\theta_k+t)}-\tan^2\gamma_k\,e^{i2t}}{i\,|\tan\gamma_k|e^{it}}\right)\\
&= -\frac{d\zeta(\dot{z}_k)^2}{2\,|\tan\gamma_k|}\operatorname{Re}(ie^{-it}-i\sec^2\gamma_k\,e^{i(2\theta_k-t)}-i2\sec\gamma_k|\tan\gamma_k|e^{i\theta_k}-i\tan^2\gamma_k\,e^{it})\\
&= -\frac{d\zeta(\dot{z}_k)^2}{2\,|\tan\gamma_k|}(\sin t+\sec^2\gamma_k\sin(2\theta_k-t)+2\sec\gamma_k|\tan\gamma_k|\sin\theta_k+\tan^2\gamma_k\sin t)\\
&= \frac{(-1)^k d\zeta(\dot{z}_k)^2}{2\sin\gamma_k\cos\gamma_k}\big(\sin t+\sin(2\theta_k-t)+(-1)^{k-1}2\sin\gamma_k\sin\theta_k\big)\\
&= \frac{(-1)^k d\zeta(\dot{z}_k)^2}{\sin\gamma_k\cos\gamma_k}\sin\theta_k\left(\cos(\theta_k-t)+(-1)^{k-1}\cos\left(\gamma_k-\frac{\pi}{2}\right)\right).
\end{aligned}$$

Similarly, we have

$$dX_2(\dot{z}_k) = \frac{(-1)^{k-1} d\zeta(\dot{z}_k)^2}{\sin\gamma_k\cos\gamma_k}\cos\theta_k\left(\cos(\theta_k-t)+(-1)^{k-1}\cos\left(\gamma_k-\frac{\pi}{2}\right)\right).$$

In case (C2), we have

$$|\tan\gamma_k| = \tan\gamma_k.$$

Hence, we compute as above to obtain

$$\begin{aligned}
dX_1(\dot{z}_k) &= -\frac{d\zeta(\dot{z}_k)^2}{\sin\gamma_k\cos\gamma_k}\sin\theta_k\left(\cos(\theta_k-t)+\cos\left(\gamma_k-\frac{\pi}{2}\right)\right),\\
dX_2(\dot{z}_k) &= \frac{d\zeta(\dot{z}_k)^2}{\sin\gamma_k\cos\gamma_k}\cos\theta_k\left(\cos(\theta_k-t)+\cos\left(\gamma_k-\frac{\pi}{2}\right)\right).
\end{aligned} \tag{15}$$

Thus, in both cases we have

$$\frac{dX_2(\dot{z}_k)}{dX_1(\dot{z}_k)} = -\cot\theta_k. \tag{16}$$

Hence, the curve $X(C_k)$ is contained in a plane parallel to the vertical plane $V_k = \{(x_1, x_2, x_3) \mid x_2 = -x_1 \cot\theta_k\}$. That $X(C_k)$ is a contact curve of contact angle γ_k follows immediately from the fact that $g(z) = z$.

Moreover, we will show that

$$\begin{aligned} &dX_1(\dot{z}_1) < 0 \text{ on } \mathring{C}_1 \text{ in both cases,} \\ &dX_1(\dot{z}_2) < 0 \text{ on } \mathring{C}_2 \text{ in case (C1),} \\ &dX_1(\dot{z}_2) > 0 \text{ on } \mathring{C}_2 \text{ in case (C2).} \end{aligned} \tag{17}$$

To see this, consider again the points $e^{i(\theta_k+\gamma_k)}$ and $e^{i(\theta_k-\gamma_k)}$ on the unit circle (see Figure 3), assume for the moment that $\gamma_1, \gamma_2 \neq \pi/2$, and define $\epsilon_k = +1$ or -1 according to whether $\tan\gamma_k$ is positive or negative — explicitly, $\epsilon_k = 1$ except for $k = 2$ in case (C1). Then

$$e^{i(\theta_k\pm\gamma_k)} = \sec\gamma_k\, e^{i\theta_k} + |\tan\gamma_k| e^{i(\theta_k\pm\gamma_k\pm\epsilon_k\pi/2)},$$

so that z_k is defined for t in an interval $[a_k, b_k]$, where

$$a_k \geq \theta_k + \epsilon_k\gamma_k + \pi/2, \quad b_k \leq \theta_k - \epsilon_k\gamma_k + 3\pi/2.$$

Hence, for z_k we have $\pi/2 + \epsilon_k\gamma_k \leq t - \theta_k \leq 3\pi/2 - \epsilon_k\gamma_k$, so that

$$\cos(\theta_k - t) + \epsilon_k \cos(\pi/2 - \gamma_k) < 0 \quad \text{on } \mathring{C}_k. \tag{18}$$

The inequalities (17) follow from (13), (14), (15), and (18). The computations when $\gamma_k = \pi/2$ for some k are similar to those above and are therefore omitted.

If some a_k is present as an edge of Ω, we parametrize it counterclockwise by $w_k(t) = e^{it}$, so that $dz(\dot{w}_k) = ie^{it}$. Recall that ζ maps a_k into a line of slope -1 for $k = 1, 3$ and slope 1 for $k = 2$ (see Figure 4). Thus, $d\zeta(\dot{w}_k)^2 = (-1)^k i\, |d\zeta(\dot{w}_k)|^2$, so that

$$\begin{aligned} dX_1(\dot{w}_k) &= (-1)^k |d\zeta(\dot{w}_k)|^2\, \tfrac{1}{2}\operatorname{Re}(e^{-it} - e^{it}) = 0, \\ dX_2(\dot{w}_k) &= (-1)^k |d\zeta(\dot{w}_k)|^2\, \tfrac{1}{2}\operatorname{Re}(i(e^{-it} + e^{it})) = 0, \\ dX_3(\dot{w}_k) &= (-1)^k |d\zeta(\dot{w}_k)|^2. \end{aligned}$$

Thus X maps a_k monotonically onto a vertical line segment in $\mathbb{R}^3$.

Finally, parametrize b from bottom to top by $z_b(t) = it$. Then $dz(\dot{z}_b) \equiv i$, and since ζ maps b into a line of slope 1, we have $d\zeta(\dot{z}_b)^2 = i\, |d\zeta(\dot{z}_b)|^2$. Computing, we have

$$dX_1(\dot{z}_b) = |d\zeta(\dot{z}_b)|^2\,\tfrac{1}{2}\,(1+t^2) > 0,$$

$$dX_2(\dot{z}_b) = |d\zeta(\dot{z}_b)|^2\,\tfrac{1}{2}\,(1-t^2)\,\mathrm{Re}(i) = 0,$$

$$dX_3(\dot{z}_b) = |d\zeta(\dot{z}_b)|^2\,t\,\mathrm{Re}(i) = 0.$$

Thus, b is mapped monotonically by ζ onto a line segment in the x-direction.

Summing up, we see that $X(\partial\Omega)$ projects onto the boundary of a triangle with interior angles α_1, α_2, $\phi = \pi - \alpha_1 - \alpha_2$ and edges s_1, s_2, b such that α_k is the interior angle of the triangle between s_k and b. The projection is one-to-one except for vertical line segments that may lie over the vertices. A sharpened version of Radó's Theorem (see [Dierkes et al. 1992]) then implies that $X(\mathring{\Omega})$ is a graph over the interior of the triangle, and we have finished the proof of Theorem 2.

References

[Ahlfors 1973] L. V. Ahlfors, *Conformal invariants: topics in geometric function theory*, McGraw-Hill Book Co., New York, 1973. MR 50 #10211 Zbl 0272.30012

[Concus and Finn 1996] P. Concus and R. Finn, "Capillary wedges revisited", *SIAM J. Math. Anal.* **27**:1 (1996), 56–69. MR 96m:76006 Zbl 0843.76012

[Crenshaw and Lancaster 2006] J. Crenshaw and K. Lancaster, "Behavior of some CMC capillary surfaces at convex corners", *Pacific J. Math.* **224**:2 (2006), 231–246.

[Dierkes et al. 1992] U. Dierkes, S. Hildebrandt, A. Küster, and O. Wohlrab, *Minimal surfaces, I: Boundary value problems*, Grundlehren Math. Wiss. **295**, Springer, Berlin, 1992. MR 94c:49001a Zbl 0777.53012

[Finn 1996] R. Finn, "Local and global existence criteria for capillary surfaces in wedges", *Calc. Var. Partial Differential Equations* **4**:4 (1996), 305–322. MR 97f:53005 Zbl 0872.76017

[Hoffman and Karcher 1997] D. Hoffman and H. Karcher, "Complete embedded minimal surfaces of finite total curvature", pp. 5–93 in *Geometry, V*, edited by R. Osserman, Encyclopaedia Math. Sci. **90**, Springer, Berlin, 1997. MR 98m:53012 Zbl 0890.53001

Received September 1, 2004.

ROBERT HUFF
DEPARTMENT OF MATHEMATICS
INDIANA UNIVERSITY
BLOOMINGTON, IN 47405
UNITED STATES
rohuff@indiana.edu